Translational

MicroRNA Profiling in Ocular Adnexal Lymphoma: A Role for MYC and NFKB1 Mediated Dysregulation of MicroRNA Expression in Aggressive Disease

Christoffer Hother,[1] Peter Kristian Rasmussen,[2] Tejal Joshi,[3] Ditte Reker,[1] Ulrik Ralfkiær,[1] Christopher T. Workman,[3] Steffen Heegaard,[2,4] Elisabeth Ralfkiær,[5] and Kirsten Grønbæk[1]

[1]Department of Hematology, Rigshospitalet, Copenhagen, Denmark
[2]Department of Neuroscience and Pharmacology, Eye Pathology Institute, University of Copenhagen, Copenhagen, Denmark
[3]Center for Biological Sequence Analysis, Technical University of Denmark, Lyngby, Denmark
[4]Department of Ophthalmology, University of Copenhagen, Glostrup Hospital, Glostrup, Denmark
[5]Department of Pathology, Rigshospitalet, Copenhagen, Denmark

Correspondence: Kirsten Grønbæk, Department of Hematology, L4042, Rigshospitalet, Blegdamsvej 9, DK-2100 Copenhagen Ø, Denmark; kirsten.groenbaek@regionh.dk.

CH and PKR contributed equally to the work presented here and should therefore be regarded as equivalent authors.

Submitted: April 22, 2013
Accepted: June 23, 2013

Citation: Hother C, Rasmussen PK, Joshi T, et al. MicroRNA profiling in ocular adnexal lymphoma: a role for MYC and NFKB1 mediated dysregulation of microRNA expression in aggressive disease. *Invest Ophthalmol Vis Sci*. 2013;54:5169–5174. DOI: 10.1167/iovs.13-12272

Purpose. Ocular adnexal lymphoma (i.e., lymphoma with involvement of the orbit, eyelids, conjunctiva, lacrimal gland, and lacrimal sac), although rare, is common among malignant tumors involving the ocular adnexal region. The main subtypes are low-grade extranodal marginal zone lymphoma (EMZL) and aggressive diffuse large B-cell lymphoma (DLBCL). In rare cases, low-grade EMZL are reported to transform to DLBCL. It is unclear, however, which genetic events distinguish low-grade disease from aggressive, potentially fatal disease.

Methods. Using LNA-based arrays from Exiqon, we performed global microRNA (miRNA) expression profiling of 18 EMZLs and 25 DLBCLs involving ocular adnexal sites to investigate changes in the miRNA expression in low- versus high-grade disease. Findings were confirmed by real-time quantitative PCR (RTq-PCR).

Results. Our analysis revealed 43 miRNAs with altered expression profiles in DLBCL compared to EMZL. Seven of the miRNAs down-regulated in DLBCL relative to EMZL showed enrichment for a direct transcriptional repression by the oncoprotein MYC. We also report a possible loss-of-regulation of NFKB1 and its downstream miRNAs. In addition, our analysis identified a group of DLBCLs whose expression profiles resembled that of EMZL. Although transformation of EMZL to DLBCL in the ocular adnexal region is rare, we hypothesize that the intermediate group potentially may derive from transformation of EMZL that was not recognized by histology.

Conclusions. We conclude that fundamental differences in miRNA expression exist between ocular adnexal EMZL and DLBCL, mainly due to differences in MYC and NF-κB regulatory pathways.

Keywords: ocular adnexal lymphoma, EZML, DLBCL, microRNA

Ocular adnexal lymphoma (OAL), found in the orbit, eyelids, conjunctiva, lacrimal sac, and lacrimal gland, is a heterogeneous group of malignancies representing 6% to 8% of extranodal non-Hodgkin lymphomas (NHL).[1,2] Although rare, OAL is the most common malignancy of the orbit.[3] Extranodal marginal zone lymphoma (EMZL) is the most frequent ocular lymphoma and is indolent in nature. By contrast, diffuse large B-cell lymphoma (DLBCL) of the ocular adnexal region (oDLBCL) is characterized by aggressive growth and poor outcome.[4] A prolonged history of ocular adnexal EMZL (oEMZL), in rare cases, may be followed by disease progression and transformation toward oDLBCL. It recently has been shown that during a 52-month follow-up, 4% of the low-grade oEMZL patient samples transformed to oDLBCL.[5] However, it is unknown how many apparently primary oDLBCLs, indeed, are preceded by an EMZL lesion, suggesting that the numbers may be higher. The molecular aspects distinguishing oEMZL from oDLBCL have not been explored in much detail, mainly due to the limited amount of diagnostic material and the requirement of fresh frozen tissue for most methods. Most previous studies of tumor suppressor pathways in lymphoma have focused on the disruption of the coding sequences of genes. However, it is evident that epigenetic alterations and aberrant expression of noncoding RNAs, such as microRNAs (miRNAs), may be equally important for disease development and transformation to aggressive forms of disease.

miRNAs are short 19 to 22 nucleotide noncoding RNA molecules that target complementary regions in the 3′UTR of protein encoding mRNAs, which may disrupt gene expression by either mRNA degradation or translational inhibition. A single miRNA may influence the expression of a large number of protein-encoding genes. Therefore, even moderate changes in miRNA expression may have great impact on tumorigenesis.[6] Several miRNAs have been linked to tumorigenesis, and they may display tumor suppressive or oncogenic features. For example, miR-16, miR-143, miR-145, and let-7 family miRNAs have tumor-suppressive effects; whereas miR-125b-1, miR-1, and miR-17-92 cluster members have been linked to tumor

proliferative or oncogenic activities.[7] Dysregulation of miRNAs, whether from genetic or epigenetic events, can lead to the loss of miRNA-mediated regulation[8] and the disrupted expression of protein-coding genes.[9]

In the present study, we compared miRNA expression patterns in oEMZL and oDLBCL using formalin-fixed paraffin-embedded (FFPE) specimens from patients suffering from these diseases. We aimed to understand the molecular mechanisms that distinguish low-grade EMZL from aggressive DLBCL, and the potential role of miRNAs in transformation by applying an integrative bioinformatics approach.

Materials and Methods

Patient Samples

This study includes diagnostic specimens from the ocular adnexal region from 25 patients with oDLBCL, and 18 patients with oEMZL. Of the 25 oDLBCLs, 15 patients presented with primary ocular adnexal lymphoma, which was defined as lymphoma involving the ocular adnexal region (Stage I) with or without involvement of unilateral preauricular, and/or submandibular lymph nodes and/or adjacent structures, such as the parotid gland (Stage II); or no prior history of lymphoma disease. Likewise, 15 of the 18 oEMZLs were primary lymphomas. The remaining cases (3 oEMZLs and 10 oDLBCLs) presented with ocular adnexal lymphoma in conjunction with lymphoma involvement elsewhere or with a recurrence involving the ocular adnexal region (secondary OAL). All oEMZLs were orbital biopsies, while the 25 oDLBCLs were from the orbit (18), lacrimal gland (3), eyelid (3), and conjunctiva (1). The FFPE specimens were retrieved from several Danish pathology departments between 1980 and 2009. For histopathologic examination, all sections were stained with hematoxylin-eosin (H&E) and analyzed immunohistochemically using the following panel of antibodies: bcl-2, bcl-6, CD3, CD5, CD10, CD20, CD23, CD79α, cyclin D1, MUM-1, and Ki-67. Two independent pathologists (ER, SH) examined and reviewed the samples, and, in agreement, classified the specimens according to the World Health Organization Classification of Tumors of Hematopoietic and Lymphoid Tissues.[10] Confirmed cases of DLBCL additionally were categorized as either germinal center B-cell–like (GCB) or non-GCB types according to the algorithm by Hans et al.[11] The study followed the tenets of the Declaration of Helsinki and was approved by the local ethics committee. The authors declare no conflict of interest.

RNA Extraction

Total RNA was isolated from four to eight 10 μm tissue sections using the RecoverAll, Total Nucleic Acid Isolation Kit (Applied Biosystems/Ambion, Carlsbad, CA) according to manufacturer guidelines. Briefly, the samples were incubated in Xylene at 50°C to remove paraffin excess, followed by ethanol washes. Proteins were degraded by digestion buffer using protease solution at 50/80°C. Samples were bound to a spin-filter by addition of isolation buffer and ethanol. DNA was degraded by DNAse treatment. The filter was washed several times and total RNA was eluted in 60 μL elution solution. Total RNA quantity and quality were checked by spectrophotometer (Nanodrop ND-1000; Thermo Scientific, Wilmington, DE).

MiRNA Microarrays

From each sample 500 ng of total RNA was labeled with fluorescent dye using the miRCURY LNA microRNA Hy3/Hy5 Power Labeling kit (Exiqon, Vedbaek, Denmark). In brief, sample RNA and reference RNA (FirstChoice Human Total RNA Survey Panel; Applied Biosystems/Ambion) was mixed with a spike-in mix containing 52 different synthetic unlabeled miRNAs and treated subsequently with calf intestinal alkaline phosphatase (CIP), to catalyze the 5′ phosphate group's removal, 30 minutes at 37°C. The CIP-treated RNA was labeled with Hy3/Hy5 by addition of labeling buffer, fluorescent Hy3/Hy5 label, DMSO and labeling enzyme, and incubated at 16°C. All samples were labeled the same day with the same master mix, in order to minimize technical variation.

The labeled samples were hybridized to miRCURY LNA arrays (v11.0; Exiqon), which contain capture probes targeting all human miRNAs registered in the miRBase version 14.0 at the Sanger Institute, as well as a selection of other small RNAs. The hybridization was performed according to manufacturer specifications using a Tecan HS4800 hybridization station (Tecan Group Ltd., Grödig, Austria). Slides were loaded into the Tecan Hybridization station and primed with ×1 hybridization buffer. A total of 50 μL of each sample was injected and the inlet flushed with 10 μL 1× hybridization buffer. Sample was hybridized to the slide at 56°C for 16 hours with medium agitation. The slides were washed several times at room temperature with wash buffers of varying salt and detergent concentrations. Finally, the slides were dried using pure nitrogen. Samples were divided randomly into 5 batches to minimize day-to-day variation in the hybridization process. After hybridization and washing, microarray slides were scanned using the Agilent G2565BA Microarray Scanner System (Agilent Technologies, Inc., Santa Clara, CA) at 5 μm resolution and the resulting TIFF images segmented using the Genepix software (version 6.1) on standard settings (Molecular Devices, Inc., Sunnyvale, CA).

Analysis of miRNA Microarrays

All microarray data processing steps were performed using the R environment.[12] The Genepix median intensities were read into R using the LIMMA package.[13] Further, the "normexp" method of background correction (with offset = 10) was applied[14] to correct for spatial biases. This step was followed by within-array normalization using the robust spline method. To reduce variance between arrays, we applied the quantile-based normalization "Rquantile."[14,15] For differential expression analysis between oDLBCL and oEMZL, only foreground intensities were used. Empirical Bayes moderated *t*-test statistics were obtained using LIMMA package.[13] *P* values were adjusted using the Benjamini-Hochberg correction method.

MiRNA Regulatory Network

Predicted and validated targets of the significantly differentially expressed miRNAs were obtained from MiRwalk.[16] Transcription factor (TF)-miRNA interactions were obtained from transmiR database.[17]

Real-Time Quantitative PCR (RT-qPCR)

MiRNAs were quantified using the miRCURY LNA Universal RT microRNA PCR kit (Exiqon) according to manufacturer's protocol. Briefly, reverse transcription (RT) was performed using 40 ng of total RNA from each sample. For quality control of the cDNA synthesis, RNA spike-in was added to each RT reaction, and later quantified using control primers included in the kit. The miRNAs let-7g, miR-16, miR-27a, miR-27b, miR-29a, miR-29b, miR-29c, miR-30e, miR-222, miR-199a-5p, and miR-1248 (nomenclature according to miRBase 17) were quantified using LNA PCR primer sets. RT-qPCR was performed using the LightCycler 480 instrument (Roche Diagnostics, Basel, Switzerland) and the conditions recommended by Exiqon. The PCR cycle crossing point (Cp) was determined for each well, and

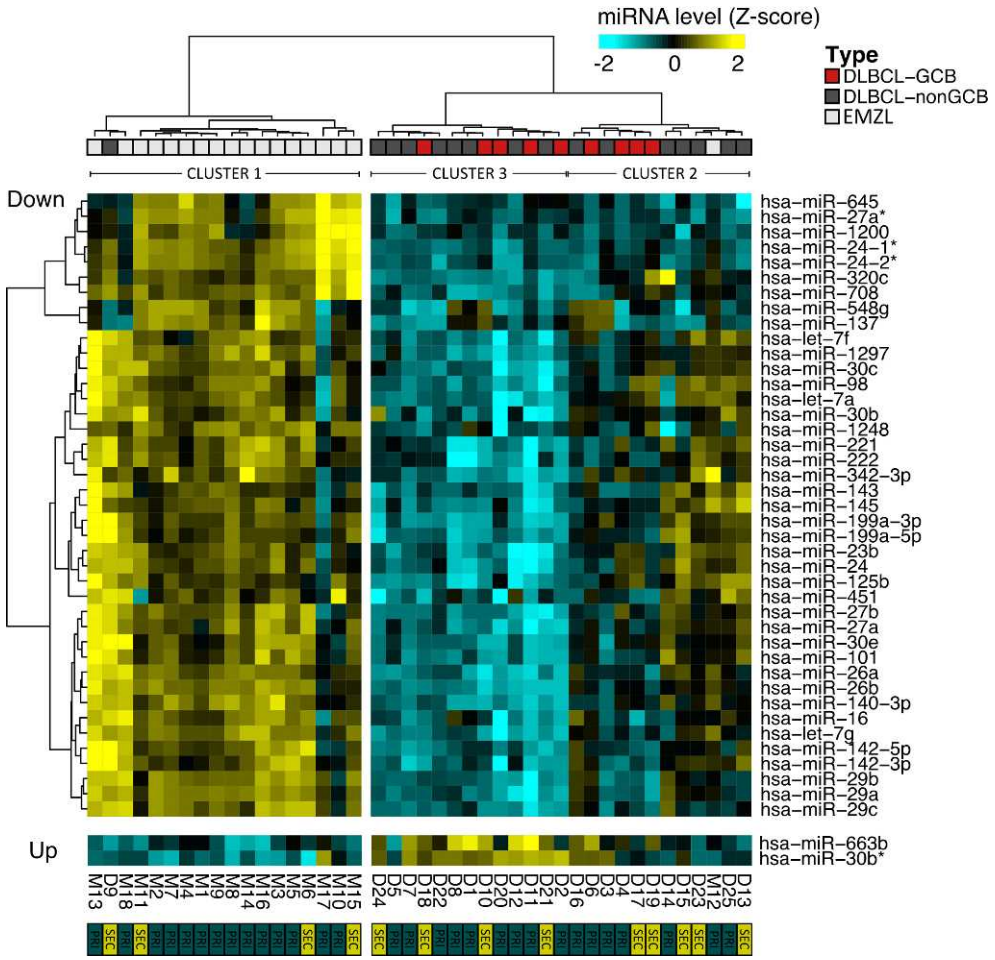

Figure 1. Two-dimensional hierarchical clustering of oEMZL and oDLBCL for the significantly differentially expressed miRNAs between oEMZL and oDLBCL. The miRNAs downregulated in DLBCL (*top section of heatmap*) show a less variable pattern across patient samples relative to the 2 miRNAs upregulated in DLBCL (*lower section of heatmap*). Cases classified according to Hans (DLBCL-GCB versus DLBCL–non-GCB), and primary ocular adnexal lymphoma (PRI) versus secondary lymphoma (SEC) were distributed randomly among these clusters.

Cp estimates from two technical replicates for each probe-set were combined to produce one signal by taking the mean of reliable wells. Cp values were tested for differences between oEMZL and DLBCL groups using empirical Bayes moderated *t*-test of the LIMMA package[13] as was done with microarray measurements. Log-fold changes were calculated by the mean Cp(oEMZL) minus the mean of Cp(oDLBCL), as to be comparable to microarray based log-fold changes.

Results

Cohort Summary

Of the 18 patients with oEMZL, 9 patients were men. The median age of the patients was 70 years (range, 26–90 years). Fifteen patients (83%) presented with Stage I lymphoma and 3 (17%) had Stage IV lymphoma. Information of treatment modalities was available for 14 patients. Of these, 12 (86%) patients were treated with radiation therapy and 2 (14%) received systemic chemotherapy without rituximab. All patients achieved complete remission and none of the patients had a relapse. The 5-year overall survival for the entire group of oEMZLs was 77%. Staging and treatment details are listed in Supplementary Table S1.

Men predominated (15/25, 60%) the group with oDLBCL. The median age was 78 years (range, 35–97 years). A total of 14 patients (56%) presented with Stage I, 3 (12%) had Stage II, 1 (4%) had Stage III, and 7 (28%) presented with Stage IV lymphoma. Of the 17 patients in Stage I/II, 15 patients had primary OAL (designated primary OAL in Fig. 1), while two patients had a localized recurrence (Stage II). Nine of the patients were classified as GCB and 16 as non-GCB type. The 25 patients were treated with combination chemotherapy (11/25, 44%); radiation therapy only (8/25, 32%); chemotherapy plus rituximab (2/25, 8%); and chemotherapy plus radiation therapy (1/25, 4%), surgery (1/25, 4%), and no treatment (2/25, 8%). Relapse or progression of disease was observed in 19 patients (76%). A total of 22 patients died during follow-up (22/25, 88%). Of these, 17 died from lymphoma progression. No patient was immunosuppressed. The 5-year overall survival for the entire oDLBCL group was 18%. The overall survival was not significantly different between primary and secondary oDLBCLs (5-year overall survival, 22% vs. 10%, log-rank $P = 0.09$). Staging and treatment details are listed in Supplementary Table S2.

Comparison of miRNA Expression Profiles in oEMZL and oDLBCL

Of the roughly 1900 RNA species included on the array, 892 human mature-miRNAs (annotated according to miRBase 16.0) were investigated in this study of 43 lymphoma samples. No

Table 1. Downregulated miRNAs for oDLBCLs Relative to oEMZL, Log-Fold Changes (LFC), and Their Associated *P* Values

miRNA	LFC	*P* Value	miRNA	LFC	*P* Value
hsa-miR-24-2*	−2.5	7.0E-44	hsa-miR-143	−0.99	1.3E-09
hsa-miR-24-1*	−2.1	7.5E-44	hsa-miR-222	−0.98	3.3E-19
hsa-miR-29a	−2.1	2.0E-31	hsa-miR-27a	−0.97	2.6E-17
hsa-miR-29b	−2.1	5.5E-28	hsa-miR-342-3p	−0.96	5.7E-15
hsa-miR-29c	−1.9	2.0E-26	hsa-miR-548g	−0.96	3.4E-05
hsa-miR-26a	−1.6	7.4E-27	hsa-miR-320c	−0.95	4.8E-20
hsa-miR-26b	−1.6	1.7E-29	hsa-miR-1297	−0.93	4.9E-24
hsa-let-7g	−1.6	6.5E-34	hsa-miR-1200	−0.9	1.0E-09
hsa-miR-140-3p	−1.3	1.0E-29	hsa-miR-137	−0.88	2.3E-05
hsa-miR-142-3p	−1.3	7.5E-17	hsa-miR-708	−0.87	4.7E-30
hsa-miR-451	−1.2	2.5E-08	hsa-miR-23b	−0.87	2.0E-10
hsa-miR-27a*	−1.2	7.4E-27	hsa-miR-27b	−0.87	2.5E-13
hsa-miR-142-5p	−1.1	5.0E-13	hsa-let-7a	−0.85	2.8E-13
hsa-miR-16	−1.1	2.4E-18	hsa-miR-145	−0.84	6.3E-11
hsa-miR-125b	−1.1	3.1E-10	hsa-miR-24	−0.83	1.9E-11
hsa-miR-30e	−1.1	2.6E-13	hsa-miR-30c	−0.82	5.8E-18
hsa-miR-101	−1.1	2.3E-16	hsa-miR-1248	−0.81	4.4E-16
hsa-miR-199a-5p	−1	5.5E-09	hsa-miR-30b	−0.8	8.9E-12
hsa-miR-199a-3p	−1	4.7E-08	hsa-miR-221	−0.79	3.9E-15
hsa-miR-645	−1	7.4E-18	hsa-let-7f	−0.74	3.2E-11
			hsa-miR-98	−0.73	3.1E-11

clear correlations were observed between the known immunostratification of the samples according to the Hans classification and the miRNA expression profiles. In addition, no relationship between miRNA expression profiles and overall survival was observed within the two histological groups (data not shown). However, differential miRNA expression analysis identified 43 significantly differentially expressed miRNAs in oDLBCL versus oEMZL, 2 upregulated, and 41 downregulated in oDLBCL relative to oEMZL (Tables 1, 2).

Hierarchical Clustering of the Significantly Differentially Expressed miRNAs

To characterize further the miRNAs that were expressed differentially between oEMZL and oDLBCLs, we performed a clustering of patients and differentially expressed miRNAs (Fig. 1). As expected, this separated oEMZL from oDLBCL samples, with the exception of two outliers. Although the analysis of histology did not reveal any characteristic features of these two tumors, the oEMZL (sample "M12") showed a higher level (>30%) of the proliferation marker KI67. The second outlier (sample "D9") was an oDLBCL that clustered with the oEMZL and, interestingly, had a relatively low proliferation marker of 30% (Fig. 1).

A more detailed analysis identified three clusters: Cluster 1, oEMZL (high expression); cluster 2, oDLBCL (intermediate expression); and cluster 3, oDLBCL (low expression). Thus, the oDLBCLs in cluster 2 seem to resemble oEMZL more than oDLBCLs in cluster 3 (Fig. 1). Interestingly, primary and secondary lymphoma were distributed randomly within the clusters, and so were non-GCB and GCB type oDLBCLs among clusters 2 and 3 (Fig. 1).

RT-qPCR–based validation was performed for 11 miRNAs found to be expressed differentially by microarray analysis: let-7g, miR-16, miR-27a, miR-27b, miR-29a, miR-29b, miR-29c, miR-30e, miR-199a, miR-222, and miR-1248. The Pearson correlation coefficients (PCC) between microarray and RT-qPCR measurements ranged from –0.67 to –0.95 ($P < 0.01$), for 10 of the 11 tested miRNAs, but was –0.28 for miR-27b. Correlation analysis can be seen in Supplementary Figure S1, and overall, these data reflect a good to excellent correlation between microarray and RT-qPCR results. More importantly, we compared the extent of differential expression observed in the RT-qPCR data compared to the microarray data (Fig. 2). The log-fold change and *P* values were highly correlated between the technologies. Ten of the 11 tested miRNAs found differentially expressed by microarray also were found to be significantly differentially expressed by RT-qPCR with miR-27b being the one exception. While the extent of significance was quite different between microarray- and RT-qPCR–based *P* values, the log-fold changes were found to be very similar in scale (Fig. 2).

Table 2. Upregulated miRNAs in oDLBCLs Relative to oEMZL, LFC, and Their Associated *P* Values

miRNA	LFC	*P* Value
hsa-miR-30b*	0.85	6.7E–09
hsa-miR-663b	0.71	5.4E–06

Discussion

Lymphomas involving the ocular adnexal region are a group of malignancies with heterogeneous clinical, molecular, and pathologic characteristics. EMZL is the most frequent type of lymphomas in the ocular adnexal region that generally is indolent, but in rare cases is reported to transform into high-grade DLBCL. In the present study, we investigated the role of miRNAs in oEMZL versus oDLBCL by miRNA expression profiling of FFPE specimens from patients suffering from these diseases.

We observed 43 differentially expressed miRNAs between oEMZL and oDLBCL samples, a majority of which (41) were found at lower levels in oDLBCL than in oEMZL. A selected set of these miRNAs was validated by RT-qPCR on all patient material. Of the 11 miRNAs for which RT-qPCR validations were performed, 10 confirmed a significant differential expression between oDLBCL and oEMZL types by RT-qPCR. Measurements from miR-29 family miRNAs, miR-222, let-7g, and miR-199-5p were highly correlated (PCC ~ –0.9) between microarray and RT-qPCR technologies in addition to exhibiting similar and significant differential expression by RT-qPCR.

The miRNAs significantly downregulated in oDLBCL included the miR-24 family of miRNAs; miR-221/222, miR-23a, and

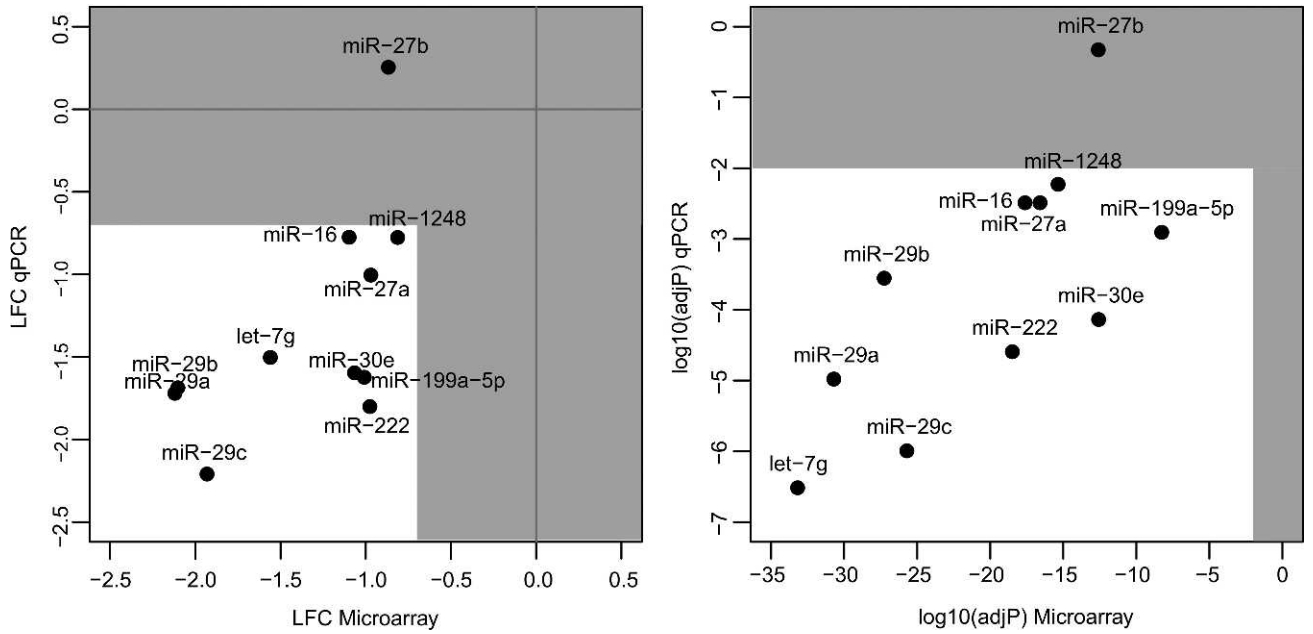

Figure 2. Comparison of RT-qPCR and microarray-based differential expression analyses (oDLBCL versus oEMZL). *Left* shows log2-fold changes (LFC) and the extent of agreement with the significance criteria, $|LFC| > 0.7$ (*white regions*). *Right* shows the comparison of log10 Benjamini-Hochberg adjusted *P* values (adjP) for the same miRNAs with significance defined by $P < 0.01$.

the miR-29 cluster. MiR-29a/c have been reported previously to be under negative transcriptional regulation by MYC and NFKB1.[18,19] We also observed a significant downregulation of other known MYC suppressed miRNAs, such as miR-26a, let-7g, and miR-221[18,20] (Fig. 3). Let-7g also is repressed by Lin28B, a protein that is transactivated by MYC, and the presence of Lin28B is a necessary and sufficient condition for MYC-mediated repression of let-7g, and does not change the expression of pri-let-7.[21] In summary, at least 7 of 41 downregulated miRNAs have been shown previously to be repressed by MYC (Fig. 3).

Recent work by Craig et al. described a correlation between MYC, miR-34a, and FOXP1 during transformation of gastric EMZL to gastric DLBCL.[22] The fraction of oDLBCL that is reported to arise from the oEMZL is exceedingly low. However, in the current study, we found a group of DLBCLs (cluster 2), whose level of MYC-related miRNA expression is intermediate between oEMZL (cluster 1) and oDLBCL (cluster 3) (Fig. 1). Thus, it could be speculated whether cluster 2 oDLBCLs have developed secondary to a preceding oEMZL lesion, which, however, was not detected by histology.

Aberrant activation of the NF-κB signaling pathway has been linked repeatedly to the aggressive forms of DLBCL.[23] Aberrant NF-κB activation in EMZL and transformed DLBCL may result from recurrent chromosomal anomalies, such *API2/MALT1* and *IGH/MALT1* translocations. Both of these translocations give rise to overexpression of MALT1, which results in hyperactivation of the NF-κB signaling pathway. However, these translocations are very rare in oEMZL and oDLBCL.[4] Nonetheless, genetic regulatory mechanisms upstream of *NFKB1*, a key gene for NF-κB signaling, also may lead to an aberrant expression and activation of the NF-κB pathway. We observed that four of five NFKB1 regulatory miRNA showed a significant downregulation in oDLBCL (let-7g, miR-199a-5, miR-26a, and miR-342-3p), suggesting a loss-of-silencing of NFKB1 due to a decrease of these miRNAs. Therefore, we hypothesized that NFKB1 expression might exhibit an increase by escaping from direct or indirect miRNA-mediated regulation.[24,25] In addition, upregulation of NFKB1 may, in turn, lead to down regulation of tumor suppressor miRNAs, like the miR-29 family (Fig. 3).

The miR-29 family, which in our study is among the most downregulated miRNAs, also is transcriptionally suppressed by YY1 (ying-yang 1, Fig. 3). YY1 is a zinc finger protein, which has been suggested to be involved in the recruitment of the polycomb repressor complex,[26] and whose overexpression has been linked to a shorter survival in DLBCL and follicular lymphomas.[27,28] Members of the miR-29 family previously have been shown to downregulate the DNA methyltransferases,[29,30] which may lead to DNA promoter hypermethylation and transcriptional downregulation. Although a global methylation analysis of our oDLBCL samples is not possible on FFPE

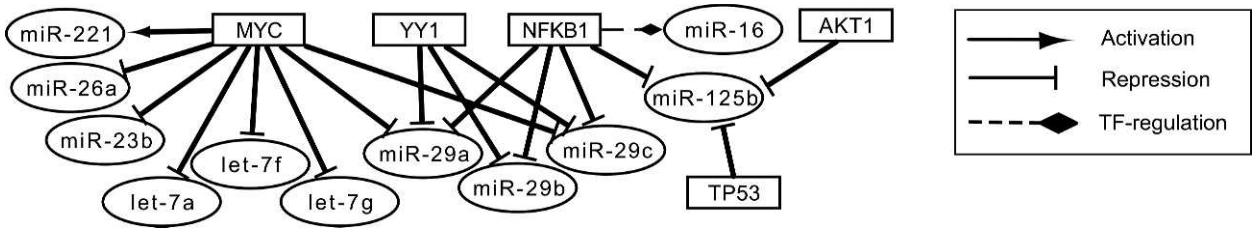

Figure 3. TF-miRNA interactions for the significantly differentially expressed miRNAs in oDLBCL targeted by MYC, YY1, and NFKB1 as curated in transmiR.

materials, due to material being degraded by this fixation process, other studies have shown that subtypes of DLBCLs show a significant hypermethylation signature.[31] The biological background for increased DNA methylation in subsets of DLBCLs is unknown at this point. *TET2* mutations may have a role in a fraction of DLBCL,[32] but this does not explain the altered methylation patterns in all cases. Additional functional studies are ongoing to solve whether downregulation of miR-29 family members leads to increased DNA methylation in DLBCL.

In conclusion, oDLBCLs showed dysregulation of miRNAs involved in the MYC and NF-κB pathways, which are general features of the most aggressive DLBCLs in other anatomic locations. This is in line with the fact that oDLBCL behave very aggressively, including the present sample population, where only 18% of patients were alive at 5 years.

Acknowledgments

Supported by grants from the Danish Cancer Society, Rigshospitalet's Research Foundation, Danish Eye Health Society, the Danish Eye Research Foundation, Synoptik Foundation, the Danish Foundation for Cancer Research, Engineer Lars Andersens Foundation, the A.P. Møller Foundation for the Advancement of Medical Science, and Merchant Kjaer and Wife Kjaer, born la Cour-Holmen's Foundation.

Disclosure: **C. Hother**, None; **P.K. Rasmussen**, None; **T. Joshi**, None; **D. Reker**, None; **U. Ralfkiær**, None; **C.T. Workman**, None; **S. Heegaard**, None; **E. Ralfkiær**, None; **K. Grønbæk**, None

References

1. Woo JM, Tang CK, Rho MS, et al. The clinical characteristics and treatment results of ocular adnexal lymphoma. *Korean J Ophthalmol*. 2006;20:7–12.
2. Freeman C, Berg JW, Cutler SJ. Occurrence and prognosis of extranodal lymphomas. *Cancer*. 1972;29:252–260.
3. Shields JA, Shields CL, Scartozzi R. Survey of 1264 patients with orbital tumors and simulating lesions: the 2002 Montgomery lecture, part 1. *Ophthalmology*. 2004;111:997–1008.
4. Sjö LD. Ophthalmic lymphoma: epidemiology and pathogenesis. *Acta Ophthalmol*. 2009;87(Thesis 1):1–20.
5. Rosado MF, Byrne GE, Ding F, et al. Ocular adnexal lymphoma: a clinicopathologic study of a large cohort of patients with no evidence for an association with chlamydia psittaci. *Blood*. 2006;107:467–472.
6. Cowland JB, Hother C, Grønbæk K. MicroRNAs and cancer. *APMIS*. 2007;115:1090–1106.
7. Esquela-Kerscher A, Slack FJ. Oncomirs: microRNAs with a role in cancer. *Nat Rev Cancer*. 2006;6:259–269.
8. Saito Y, Liang G, Egger G, et al. Specific activation of microRNA-127 with downregulation of the proto-oncogene BCL6 by chromatin-modifying drugs in human cancer cells. *Cancer Cell*. 2006;9:435–443.
9. Baylin SB, Jones PA. A decade of exploring the cancer epigenome – biological and translational implications. *Nat Rev Cancer*. 2011;11:726–734.
10. Swerdlow SH, Campo E, Harris NL, et al. *WHO Classification of Tumours of Haematopoietic and Lymphoid Tissues*, 4th ed. Lyon, France: IARC Press; 2008.
11. Hans CP, Weisenburger DD, Greiner TC, et al. Confirmation of the molecular classification of diffuse large B-cell lymphoma by immunohistochemistry using a tissue microarray. *Blood*. 2004;103:275–282.
12. R Development Core Team. *R: A Language and Environment for Statistical Computing*. Vienna, Austria: R Foundation for Statistical Computing; ISBN 3-900051-07-0, 2008. Available at: http://www.R-project.org.
13. Smyth GK. Limma: linear models for microarray data. In: Gentleman R, Carey V, Dudoit S, et al., eds. *Bioinformatics and Computational Biology Solutions Using R and Bioconductor*. New York, NY: Springer; 2005:397–420.
14. Ritchie ME, Silver J, Oshlack A, et al. A comparison of background correction methods for two-colour microarrays. *Bioinformatics*. 2007;23:2700–2707.
15. Smyth GK, Speed T. Normalization of cDNA microarray data. *Methods*. 2003;31:265–273.
16. Dweep H, Sticht C, Pandey P, Gretz N. Mirwalk-database: prediction of possible miRNA binding sites by "walking" the genes of three genomes. *J Biomed Inform*. 2011;44:839–847.
17. Wang J, Lu M, Qiu C, Cui Q. Transmir: a transcription factor-microRNA regulation database. *Nucleic Acids Res*. 2009;38:D119–D122.
18. Chang TC, Yu D, Lee YS, et al. Widespread microRNA repression by MYC contributes to tumorigenesis. *Nat Genet*. 2008;40:43–50.
19. Mott JL, Kurita S, Cazanave SC, et al. Transcriptional suppression of miR-29b-1/miR-29a promoter by c-MYC, hedgehog, and NF-kB. *J Cell Biochem*. 2010;110:1155–1164.
20. Sander S, Bullinger L, Klapproth K, et al. MYC stimulates EZH2 expression by repression of its negative regulator miR-26a. *Blood*. 2008;112:4202–4212.
21. Chang TC, Zeitels LR, Hwang HW, et al. Lin-28b transactivation is necessary for MYC-mediated let-7 repression and proliferation. *Proc Natl Acad Sci U S A*. 2009;106:3384–3389.
22. Craig VJ, Cogliatti SB, Imig J, et al. MYC-mediated repression of microRNA-34a promotes high-grade transformation of B-cell lymphoma by dysregulation of FOXP1. *Blood*. 2011;117:6227–6236.
23. Lenz G, Staudt LM. Aggressive lymphomas. *N Engl J Med*. 2010;362:1417–1429.
24. Iliopoulos D, Hirsch HA, Struhl K. An epigenetic switch involving NF-kB, lin28, let-7 microRNA, and IL6 links inflammation to cell transformation. *Cell*. 2009;139:693–706.
25. Garzon R, Pichiorri F, Palumbo T, et al. MicroRNA gene expression during retinoic acid-induced differentiation of human acute promyelocytic leukemia. *Oncogene*. 2007;26:4148–4157.
26. Woo CJ, Kharchenko PV, Daheron L, Park PJ, Kingston RE. A region of the human HOXD cluster that confers polycomb-group responsiveness. *Cell*. 2010;140:99–110.
27. Sakhinia E, Glennie C, Hoyland JA, et al. Clinical quantitation of diagnostic and predictive gene expression levels in follicular and diffuse large B-cell lymphoma by RT-PCR gene expression profiling. *Blood*. 2007;109:3922–3928.
28. Wang H, Garzon R, Sun H, et al. NF-kB-YY1-miR-29 regulatory circuitry in skeletal myogenesis and rhabdomyosarcoma. *Cancer Cell*. 2008;14:369–381.
29. Garzon R, Liu S, Fabbri M, et al. MicroRNA-29b induces global dna hypomethylation and tumor suppressor gene reexpression in acute myeloid leukemia by targeting directly DNMT3a and 3b and indirectly DNMT1. *Blood*. 2009;113:6411–6418.
30. Zhao JJ, Lin J, Lwin T, et al. MicroRNA expression profile and identification of miR-29 as a prognostic marker and pathogenetic factor by targeting CDK6 in mantle cell lymphoma. *Blood*. 2010;115:2630–2639.
31. Martín-Subero JI, Kreuz M, Bibikova M, et al. New insights into the biology and origin of mature aggressive b-cell lymphomas by combined epigenomic, genomic, and transcriptional profiling. *Blood*. 2009;113:2488–2497.
32. Quivoron C, Couronné L, Della Valle V, et al. *Tet2* inactivation results in pleiotropic hematopoietic abnormalities in mouse and is a recurrent event during human lymphomagenesis. *Cancer Cell*. 2011;20:25–38.